[redacted]

Norden

UA

DIVISION OF UNITED AIRCRAFT CORPORATION

NORWALK, CONNECTICUT

QUARTERLY PROGRESS REPORT

CONTRACT NAS8-30738

LASER SPACE RENDEZVOUS

AND DOCKING TRADE-OFF

TABLE OF CONTENTS

ABSTRACT

Under existing contract NAS8-30738, Norden is presently configuring a spaceborne LADAR sensor which will meet the requirements for rendezvous and docking with a cooperative object in synchronous orbit. The sensor is being configured around a pulsed CO_2 laser which can be constructed and deployed using technology which presently exists or is being developed, and which appears to lend itself very well to the envisioned family of space missions. In order to determine the applicability of the type of sensor being considered, the performance of a family of candidate sensors is being traded off as a function of size, weight, and power consumption. The maximum ranges being considered are 50, 100, 200, and 300 nautical miles.

Investigations which have been performed to date seem to support the original contention that a laser space rendezvous and docking sensor can be constructed within the framework of the present state-of-the-art, and will offer a cost effective and reliable solution to the presently envisioned space rendezvous requirements.

SUMMARY

The effort to date has concentrated on the identification of detailed requirements, the configuration of a family of baseline systems, and the identification of the technologies which are involved in the realization of these system configurations. As a result, the following progress has been made:

1. A baseline system configuration has been derived. This has been accomplished in such a fashion as to expedite the derivation of a final system configuration when the final rendezvous requirements are available.

2. A system block diagram which breaks out the functional subsystems has been generated.

3. A system description which describes the operation of the rendezvous and docking system, and the interaction of the various subsystems has been prepared.

4. The optical design has been substantially completed. The result is a reflective telescope, which has the capability to scan over the required area. The telescope design has called extensively on existing technology, yet has numerous features which require additional development in order to insure that the smallest, lightest, most functional design will be ultimately deployed.

5. A scan pattern has been determined which permits the beam to be scanned in an operationally functional manner, yet is compatible with the optical system.

6. The performance of the scanning LADAR has been determined as a function of range and retroreflector configuration. A parametric determination of range, retroreflector size, and required power has been made. As the maximum range requirements are reduced, the laser power, and detector array size are correspondingly reduced. This trade-off information is presented in graphical form.

7. A technique in which the basic CO_2 scanning LADAR can be utilized for the final docking maneuver has been investigated.

SYSTEM OPERATION

The system operation is broken into acquisition, tracking, and docking. During acquisition, the laser beam is slewed, via the steering mirrors, to the center of the search angle which has been designated. The transmit scanning mirror scans the beam in the preprogrammed scanning pattern, and the receive mirror scans synchronous with the transmit mirror, but out of phase by an amount necessary to allow for detection in the designated range interval only. When the return indicates a location for the target, the scanning ceases, the beam is returned to the target location, and tracking commences.

When the vehicle is within approximately 500 feet of the target, the docking is initiated. Docking involves circling the target until a pattern of reflecting and nonreflecting areas are recognized, and using certain of the characteristics of this surface, which is being designed for this specific application, to align the vehicle with the docking mechanism. A preliminary block diagram of the system is shown in Figure 1.

DETECTION PROBABILITY

In order to calculate the probability of detecting a cooperative target, the following assumptions have been made:

1. A solid angle of 5°x5° must be searched in a frame period of 10 seconds.
2. The target is equally likely to occur in any part of the solid angle which has been designated.
3. The range uncertainty is 20% of the designated maximum range.

When these assumptions are made, the detection probability becomes substantially independent of the scan pattern, and the latter can therefore be chosen as a function of mechanization convenience only. The probability of detection can be evaluated most conveniently by averaging over the ensemble of possible target positions.

Let f designate the PRF
T, the frame period
β, the 3 dB optical beamwidth
Ω, the solid angle to be searched
p, the probability of detection for a direct hit (peak of the beam).
P, the composite probability of detection for the entire frame period
p_{fa}, the probability of false alarm per pulse
N_{fo}, the total number of false alarms for the entire frame period.

A design goal is T<10 seconds;

$P = 0.98$

$P_{fa} = 10^{-4}$: for a PRF of f=5000 Hz,

this is equivalent to $N_{fa} < P_{fa} \text{TxPRF}$

$= 50$

$\beta = 0.33$ milliradian

$\Omega = 5x5x(\frac{\pi}{180})^2 = 7.6x10^{-3}$ steradians

The solid angle subtended by a beam is

$\omega_B = \frac{\pi\beta^2}{4} = 8.6x10^{-8}$ steradians

In T seconds, the solid angle illuminated can be approximated by:

$\Omega_B = \text{TxPRFx}\omega_B$,

and the ratio $\frac{\Omega_B}{\Omega} = \frac{\text{TxPRFx}\omega_B}{7.6x10^{-3}}$.

For the values chosen, this ratio is

$\frac{\Omega_B}{\Omega} = \frac{50000x8.6x10^{-8}}{7.6x10^{-3}} T = 0.565T.$

For T=10 seconds, the average point in the search field will be illuminated between 5 and 6 times.

If the probability of detection <u>per pulse</u> is designated as p_d, one can write:

$P = 1 - (1-p_d)^{\frac{\Omega_B}{\Omega}}$

Solving for p_d:

$p_d = 1-(1-P)^{\frac{\Omega}{\Omega_B}}$

For $\frac{\Omega_B}{\Omega} = 5.65$ one finds $p_d = 0.50$.

The signal-to-noise ratio, S/N, required to obtain a single pulse probability of detection $p_d=0.50$ with a false alarm ratio $p_{fa}=10^{-4}$ is given by the standard radar design curves as S/N=9.4 dB. The required transmitter average power is given by:

$$P_T = \frac{S/N(4\pi)^3 R^4 L\ P_n}{G^2 \lambda^2 \sigma \eta}$$

where

P_T = 5 to 20 watts (average transmitted power)

G = aperture gain $\cong \frac{4\pi}{\beta^2} = \frac{4\pi x 10^6}{(0.33)^2} = 1.15x10^8$

λ = $1.06x10^{-5}$ m

σ = $3.2x10^5$ m^2 for a 3" corner reflector

or $5x10^6$ m^2 for a 6" corner reflector

(in general $\sigma = 4\frac{(.289)^2 L^4}{\lambda^2}$)

R = range, in m

L = optical loss; for an efficiency of 15%, $L = \frac{1}{0.15} = 6.7$

η = quantum efficiency = 0.5

P_n = minimum detectable power, in watts

$$P_n = 2\frac{hc}{\lambda}\Delta f$$

$h = 6.6 \times 10^{-34}$ watts

$c = 3 \times 10^{8}$ ms^{-1}

Δf = bandwidth imposed by range rate uncertainty or by pulse width.

- Doppler bandwidth corresponding to range rate uncertainty

$\Delta v = 20$ ft/s : $\Delta f_D = \frac{2\Delta v}{\lambda} = \frac{2 \times 20 \times 0.305}{1.06 \times 10^{-5}} = 11.5$ MHz

- Δf_p corresponding to pulse width $T_p = 0.36$ μs

$\Delta f_p = \frac{1}{T_p} = \frac{1}{.36 \times 10^{-6}} = 2.8$ MHz

Conclusion: use $\Delta f_p = 3 \times 10^{6}$ and use a receiver consisting of four such bands. This results in a value $P_n = 1.1 \times 10^{-13}$ watts.

The required power was calculated for various detection ranges, and sizes of corner reflectors and is shown in Table I.

Since the gain of the system improves with the fourth power of the corner reflector size, at no apparent significant penalty in weight, it is desirable to use the largest practical size of corner reflector the 300 nautical miles system. This results in a power requirement of 6 watts.

TABLE I.

AVERAGE POWER REQUIREMENTS

RANGE (n.mi.)	SIZE OF SATELLITE CORNER REFLECTOR (inches)	P_{ave} watts)
300	3	92
	4	30
	5	12
	6	6
200	3	18
	4	6
	5	3
	6	1
100	3	1
50	3	0.1

OPTICS

Infrared laser radiation provides an attractive alternative to conventional radar for space applications, since diffraction effects are so much smaller with the former (by a factor equal to the ratio of the wavelengths). Angular spread of 10.6μ laser beams, for example, can be theoretically held to about 1/3mr with only a 78mm (3 in) aperture, whereas equivalent concentration of power in a radar beam of several millimeters wavelength would require an aperture of many meters.

A laser radar (LADAR) system can be designed which emits powerful coherent pulses in a given direction and detects signals reflected by a target. This direction can be changed continuously by mirrors or other means, so that a section of space may be scanned.

Heterodyne detection is extremely efficient, and can greatly reduce the laser power required to cover a given range. This is implemented by combining at the detector the returning pulse and a constant coherent beam of slightly different wavelength. The interfering coherent waves then produce a "beat" frequency which can be detected, and different pulses can be coded by varying the emitter frequency in a predetermined pattern. Cooperative targets are equipped with retroreflectors, so that laser power is minimized and coherence of the reflected beam is assured.

Design Considerations

The transmitted laser radiation must be expanded to a diameter of about 76mm, and projected in a collimated beam with about 1/3mr

divergence or less at 50% relative intensity. The returning pulses must be brought to focus at the appropriate detector position, where they are combined with the similarly focussed reference beam from the local oscillator. The optics and detection and scanning system required to achieve this are subject to many constraints, the most important of which are weight, power consumption, maintenance of coherence, optical efficiency, efficiency of the detector and its cooling system, and efficiency of the scanning system. In carrying out the design, techniques, components, and materials used are constrained by what can be confidently predicted to be technologically feasible in 1980.

Weight And Power Consumption

It is essential that the system be as light as possible since it must be launched into orbit and maneuvered through space. Every additional pound of payload represents an enormous expenditure of fuel and an equivalent launch cost of thousands of dollars. Hence, every aspect of the design must be approached from the point of view that system weight must be minimized. Power consumption must also be kept low, in order to reduce the weight of the power supply.

Coherence

Since the detection approach is based on optical interference, the system must be designed in such a way that sufficient coherence is maintained in the pulses throughout the entire trip from laser to target to detector. When a single optical channel is used for both transmitting and receiving, beamsplitter and antireflection coatings should be avoided, since they tend to cause backscatter into the

detector from the transmitting laser. This can defeat the heterodyne detection technique.

Optical Efficiency

The system should utilize as few elements as possible, both to save weight directly, and to minimize losses due to absorption, scattering, and undesired surface reflections. Such losses would require greater laser power for a given range, thus increasing the weight of both the laser and the power supply. Simple beamsplitters should be avoided since their round-trip efficiency is less than 25% and backscattered radiation error ruins heterodyne detection. Image aberrations should be reduced below the diffraction limit.

Detector/Cooler Efficiency

A detection system must be incorporated with a compatible cooling system to achieve maximum efficiency and reliability with minimum weight and power consumption. The useful lifetime of the cooling system should be sufficiently long for all proposed missions . . . at least several months.

Scanning Efficiency

A scanning technique must be chosen which enables the system to search a 30° cone in space, by covering 5° x 5° sectors in about 5 seconds. If necessary, scanning speed can be sacrificed somewhat in order to meet more important design objectives, but the time for a 5° scan should be kept below 10 seconds.

System Design

In the system actually designed, careful consideration has been given to all the factors discussed under design considerations. In order to save

considerable weight and reduce alignment difficulties, a single channel is used for both transmission and reception. This section discusses the design configuration and the reasons for the types of components and methods utilized.

Configuration

Figure 2 shows the system components listed in Table II, consisting of a local oscillator laser situated beneath the transmitting laser (both nominally 10.6μ wavelengths), all necessary optics, including a complex beamsplitter with an associated retardation plate, and a detector array in a radiation cooler. These components are discussed in the following sections on optics, detection and scanning.

Optics

Common Transmitting/Receiving Optics

The attempt to use the same optical channel for both transmitted and received radiation seems at first to run counter to the intention to avoid the large scattering and efficiency losses associated with ordinary beamsplitters. This difficulty is circumvented by utilizing an efficient Brewster angle window to distinguish between incoming and outgoing radiation. Pulses emerging from the laser are linearly polarized perpendicular to the plane of incidence at the beamsplitter. By orienting the system so that the angle of incidence is Brewster's angle, (about 70° for the material here used), about 68% of this radiation is reflected. It then passes through a retardation plate, (nominally a quarter-wave plate), and emerges circularly polarized. Upon returning, it is further retarded by the plate, and becomes linearly polarized in the plane of incidence of the Brewster angle

window. Practically all of this radiation then passes through the window, since it is incident at Brewster's angle. The round-trip efficiency of such a beamsplitter can be conservatively estimated to be at least 65%.

Beam Expander

Configuration Tradeoffs

In order to achieve the desired concentration of power in the transmitted beam, divergence must be held to about 1/3mr. If this were the angular width of the entire first order of diffraction, (the "Airy disc"), the minimum aperture diameter would be, (for λ = .0106mm),

$$D = 2.44\ \lambda/\theta = 77.6\text{mm}$$

Since the requirement is that divergence at the 50% relative intensity levels be 1/3mr or less, some margin is allowed for geometrical aberration. The latter, however, are held considerably lower than the permissible limit, so that fabrication tolerances need not cause unacceptable performance.

The need to minimize image aberrations while maintaining high transmission efficiency with as few optical elements as possible, points inexorably toward a reflecting system. A single spherical mirror can have far less spherical aberration than a lens of equivalent focal length and diameter, and so several lenses might be required to equal the performance of one mirror for small field angles. Surface scatter and reflection losses, and absorption in the lenses themselves, would also cause much greater inefficiency and loss of coherence than would a reflecting surface. It is therefore desirable

that the optical system be reflective rather than refractive wherever possible.

Due to the small size of the detectors, and the fact, (as will be discussed below,) that several are utilized in a linear array, the returning pulses must be focussed so that most of their power is concentrated on the appropriate detector. Thus, the beam expander has been designed as a focussing telescope, to avoid using additional optical elements. The transmitting laser therefore, must radiate as a point source, rather than emitting collimated wavefronts. This is entirely feasible even with today's technology.

In any telescope design, specification of the desired magnification and aperture forces the designer to trade off the working relative aperture against the allowable length and complexity of the optics, using image quality as a criterion of acceptability. Since magnification must also be traded off against length and other physical constraints, (and since excessive length results in excessive structural weight), the range of simple reflective configurations which can satisfy the system requirements, (particularly the field of view), is limited.

The system type chosen is a modification of the classical Gregorian telescope. It consists of two confocal ellipsoidal mirrors of differing focal length and eccentricity. The angular magnification of the telescope is 10, and it works internally at a relative aperture of f/2.8. The solid angle of the image cone is equivalent to a relative aperture of f/13.78, (i.e., the cone angle is 4.16°). The effective focal length of the system is 1.05 meters,

and its field of view to space is 1°. The maximum geometrical aberration is less than 1/4mr anywhere in the field, even at 100% modulation; for 50% of the power, this angular spread is reduced to less than 1/8mr. The significant optical design parameters are listed in Table III.

A characteristic of reflective designs which cannot be overlooked is that the image is formed in object space. In order to circumvent this problem, either direct occlusion is permitted, or some radiation passes through a hole in one or more mirrors, or beamsplitters must be used. In this system, the use of folding mirrors with central apertures has been chosen as the most effective method. The size of the central hole is determined both by the diameter of the converging light cone at the mirror location, (this is dominant for the pointing mirror), and by the angular field within the system (this dominates for the folding mirror at the telescope focal plane, where the primary mirror forms an image). The field of view is therefore limited by the efficiency which is accepted for these mirrors. The latter can be estimated approximately by the ratio of usable mirror area to its total area including the hole. In the design chosen, the field of view is 1°, and the "efficiency" of each mirror is at least 75%, since each central aperture represents no more than half the diameter of its associated mirror.

Materials

An important decision in the design of this system is the choice of beryllium for the mirrors. This enables the production of extremely light but rigid elements which can have very high reflectivity (>98%)

even when uncoated, or which can be coated to yield 99.4% reflectivity. The weight of such elements can be less than 1/3 that of conventional lightweight glass mirrors; by 1980, this discrepancy may be even wider. Even with the factor of 3, however, the weight of all mirrors in the system is less than 1/3kg, rather than about 0.9kg for glass.

Mounting and housing for the entire system is also envisioned to be of beryllium, both for minimization of weight, and to attempt to keep thermal expansion as uniform as possible. The mechanical housing must be constructed in such a way that in spite of thermal expansion or contraction over the expected temperature range, the common focal point of the two converging mirrors will remain confocal, and the laser source and detector positions will remain at the focus of the entire system.

Unfortunately, raw beryllium is known to have anisotropic thermal expansion properties, largely due to its hexagonal crystal structure. Several years ago, this drawback alone could have excluded the element for consideration in such an optical system. Today, however, enormous progress has been made toward being able to make this characteristic more uniform, and research and development are continuing at a strong pace. It is confidently expected that by 1980, the manufacture and working of beryllium with nearly isotropic thermal properties will have become routine. Even today, in fact, similar housings for optical systems have been made and qualified for space use. Other earlier difficulties with beryllium, such as its tendency to corrode in chloride environments, the toxicity of its dust when inhaled, the difficult of polishing it, etc., have all been overcome

with good manufacturing processes, even today. At present, for example, it takes only about twice as long to polish a mirror of beryllium as one of glass.

A more fundamental difficulty, however, lies with the manner in which linearly polarized radiation is reflected from metallic surfaces. Unless the polarization direction is either parallel or perpendicular to the plane of incidence, slightly elliptical polarization is produced. A similar effect occurs for circularly polarized light. This in turn leads to a loss of transmission efficiency when the returning pulse arrives at the Brewster angle window, since the retardation plate then transforms nearly circularly polarized radiation to nearly linearly polarized radiation. In the present system, however, the incident angles are sufficiently small that this effect is acceptable. The round-trip efficiency of the Brewster angle window due to this factor is estimated to be at least 80% of that which it would exhibit for perfectly linearly polarized radiation. In order to avoid this loss, all mirrors must be coated with dielectric reflection coatings, rather than being left bare, or coated with metals such as aluminum or gold.

Not many materials are available for 10.6μ retardation plates. Cadmium sulfide is one of these, and its internal transmission is acceptable (>99%) for short optical paths up to 3 or 4mm.

It is desirable that the Brewster angle window have a high refractive index, since this is the condition for high reflectivity of perpendicularly polarized radiation at the Brewster angle. On the other hand, germanium and silicon, which have very high indices, are subject to thermal runaway; i.e., their transmissibility is

reduced significantly when their temperature rises too high. The material chosen for this design is gallium arsenide. Its thermal stability and transmittance at 10.6μ are good, and its refractive index of 3.25 is high enough to allow 68% reflection of perpendicularly polarized light incident at Brewster's angle.

Detection

Detector Type

The choice of detector is constrained by the necessity for high sensitivity and quantum efficiency at the wavelength of interest (10.6μ), high response and decay speeds, (so that the intermediate frequency beats can be detected), and an operating temperature which can be attained without heavy, power-consuming equipment. At present, these requirements can be satisfied by mercury-cadmium telluride detectors, which can be cooled by radiation into space. Such detectors manufactured by S.A.T., (a French corporation), can be operated at temperatures of 120°K,and provide quantum efficiencies of about 30%. They can respond to frequencies in the region of 10^9Hz, which is considerably higher than necessary for this system. Research and development are continuing, both on this detector type and on lead-tin telluride junctions, which can be made with similar properties. It is expected that by 1980, 50% quantum efficiencies will be routinely attainable, perhaps even with operation at higher temperatures.

Interference

Heterodyne detection requires that the returning pulse be interfered with the beam from the local oscillator laser through the mixing beamsplitter (which should be only 1% reflective). This is

achieved by means of a holographic optical element which focusses the beam on each detector in the array simultaneously. Since the hologram cannot be easily recorded with 10.6μ radiation, it can be made at a much shorter wavelength, (for example, 0.53μ or 0.6328μ), with appropriate distortion calculated when setting up the initial configuration. Alternatively, the hologram can be generated by photographic reduction of computer-generated plots. While the latter technique is difficult for holograms in the visual region, (largely due to limited plotter accuracy, but also because of photographic aberrations), the required resolution on the material is far lower at 10.6μ. This technique is therefore feasible even today, for holograms at that wavelength, as long as the required field angles and relative aperture are not large.

Scanning

The field of view of the optical system is 1° in space. Due to the angular magnification of the beam expander this corresponds to a scanning angle of 10° at the laser. Originally, it had been hoped that this could be achieved with a mirror rotated by a piezoelectric device, but it was found that the angle was much too large. A multi-faceted mirror was then considered, but this idea was rejected due to the large weight and correspondingly high power consumption of such a component (which would have 72 facets!) Furthermore, the requirement for non-reflecting spaces between facets, (in order to avoid directional ambiguity resulting from the straddling of two facets by the beam), would cause an unacceptably large percentage of "dead time" during scanning.

The scanning system chosen for the design is remarkably simple and light in weight, and consumes very little power. It consists of a small mirror mounted on a torsion rod, which rotates sinusoidally at a fixed frequency. Such devices are presently made by Bulova, and can easily scan the 10° angle at high frequencies (up to 2000Hz, if a 7mm square mirror can be accepted; slower frequencies for the larger mirrors used in this system.) They weigh less than 40 grams, and consume less than 500mw of power.

Since the field of view is 1°, and the effective focal length of the system is 1.05m, the diameter of the image is 18.33mm. For linear scanning, a linear array of detectors would be required to cover this length. If each detector were 0.35 in diameter, (to correspond to the size of the focussed spot), and separated by 0.05mm from its neighbor, a linear array of 46 detectors would be required. This would result in too much heat for the radiation cooler to dissipate at less than 120°K, even with an increase in size and weight. A second synchronized scanning mirror is therefore included, (with its angle offset from that of the transmitting scanner, to compensate for the finite speed of light), so that pulses returning exactly from a target whose range is known require only one detector. In fact, several detectors are actually used, in order to allow detection of the target when its range is only approximately known, but this number can be reduced to about six or eight, depending upon the uncertainty in range. This number of detectors can be easily handled by radiation cooling.

Concluding Remarks

An optical design has been presented for use in a 10.6μ laser radar in space. Most aspects of the design are technologically

feasible today, and all are expected to be routinely attainable before 1980.

A single optical system has been employed for both transmitting and receiving, yet no beamsplitter coatings (with their inherent scattering properties) have been allowed in the transmitting channel. Only one component, (the retardation plate), is entirely transmissive, (thereby requiring antireflection coating on both sides), so that pactically no transmitted radiation can leak into the receiver channel without traveling to the target. (Only that reflected after passing through the retardation plate can be transmitted through the beamsplitter, and this can be reduced nearly to zero, since the coating need be designed only for a single wavelength. If even this minute level is found to cause difficulty, it can be completely eliminated by destructive interference with part of the transmitted component, simply by aligning a surface of low reflectivity at the position of detector P. That detector can then be placed in the path of that portion of the perpendicularly polarized radiation which initially passes through the Brewster angle beamsplitter.)

The overall round-trip optical efficiency of the main channel can be higher than 22%, distributed as in Table IV. assuming the acceptability of a germanium Brewster angle beamsplitter. If higher index materials are found suitable for this component, the efficiency can be even higher, but the required angle of incidence will increase accordingly.

The weight of the optical components is estimated to be about 340 gm, (¾lb) distributed as in Table II. To this must be added the weight of the

radiation cooler, estimated at 1.4 kg (3 lb), the lasers, the power supply, the motors, and all necessary baffling, mounting, and housing.

Today's technology allows a linear array of mercury-cadmium telluride detectors to the used for the heterodyne detection, since they can provide the high quantum efficiency and response speed required, even when cooled to 120°K (rather than 77°K, as required only a few years ago). The technology of 1980, however, will allow the substitution of lead-tin telluride arrays, which promise better uniformity and higher reliability at lower cost, with no loss of efficiency or speed.

The proper operating temperature has been provided in this design by a radiation cooler similar to those presently manufactured by Arthur D. Little, Inc. Practically no power is consumed by this component, and its lifetime is virtually unlimited compared to that of systems which require solid or liquid coolants.

Finally, the system as shown in Figure 1 has been designed to be relatively light and compact with a 1° field of view. If this field can be reduced, (which requires longer scanning time for a given total field, when pointing mirror speed is fixed), the optical efficiency can be improved by reducing the diameter of the hole in the focal plane folding mirror (component D). A similar improvement can be realized if the aperture can be reduced, since the telescope magnification can then decrease; however, greater beam divergence will result, due to the larger diffraction angle which results. Many other tradeoffs are possible, including increasing system focal length, (which makes the laser axes parallel to the optical axis between components B and C, but

requires larger detectors to maintain the same efficiency at the focussed image), increasing the index of the Brewster angle beamsplitter, (which improves its reflective efficiency, but requires a higher incident angle, and therefore a longer beamsplitter and optical path for a given cone angle), and placing the retardation plate at the retroreflectors on the target (which would require many such plates rather than one, and would lead to some inefficiency due to the production of elliptical polarization at oblique angles, but would completely eliminate the leakage of radiation from transmitter channel to receiver channel.) In addition, the scanning and folding mirrors and beamsplitters can be modified angularly to meet specific packaging requirements; the radiation cooler, for example, can be made to point in another direction. The optical design as presented represents a reasonable combination of tradeoffs, but is flexible enough to accommodate reoptimization for different conditions.

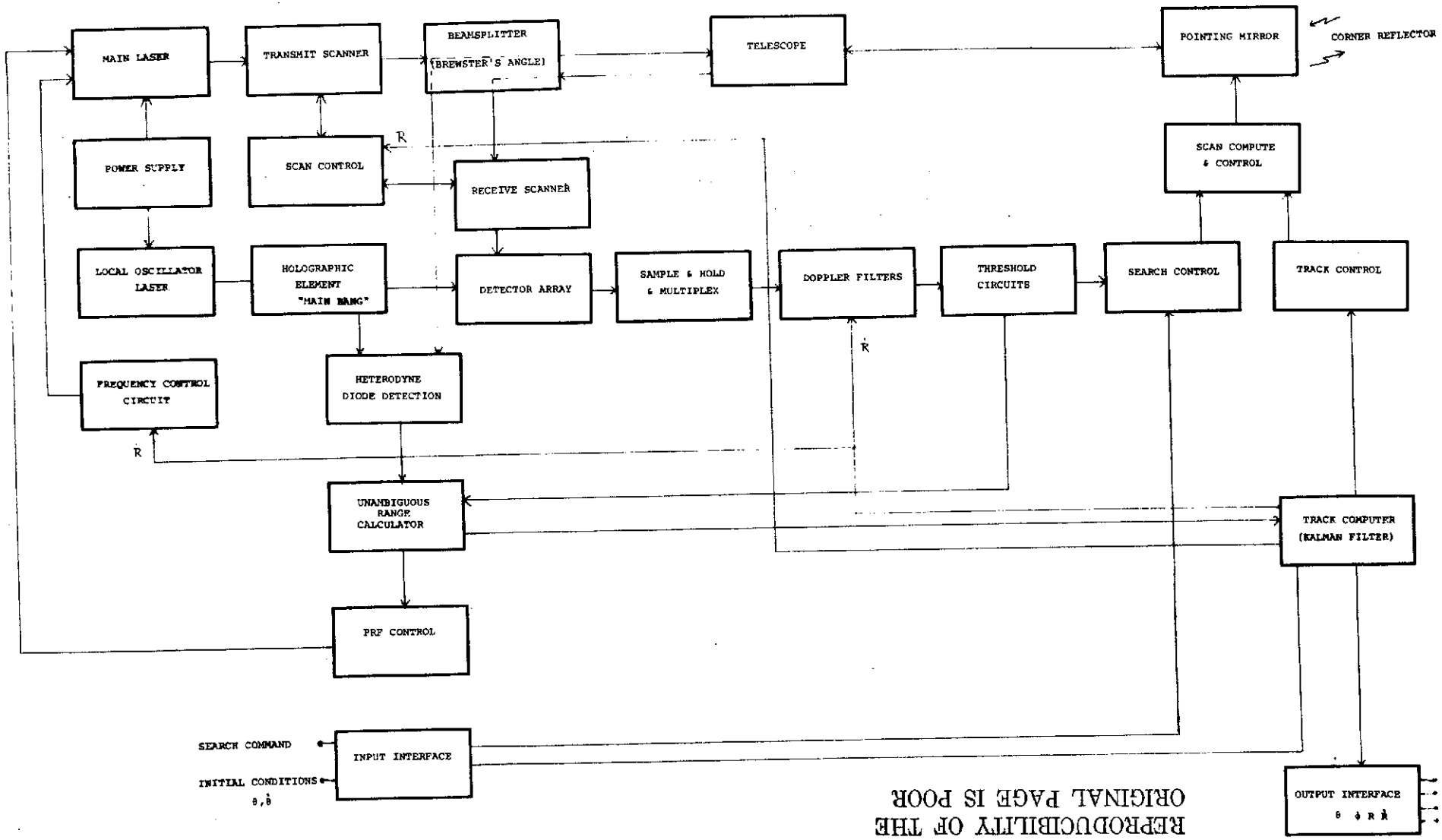

GENERAL SYSTEM BLOCK DIAGRAM

Figure 1

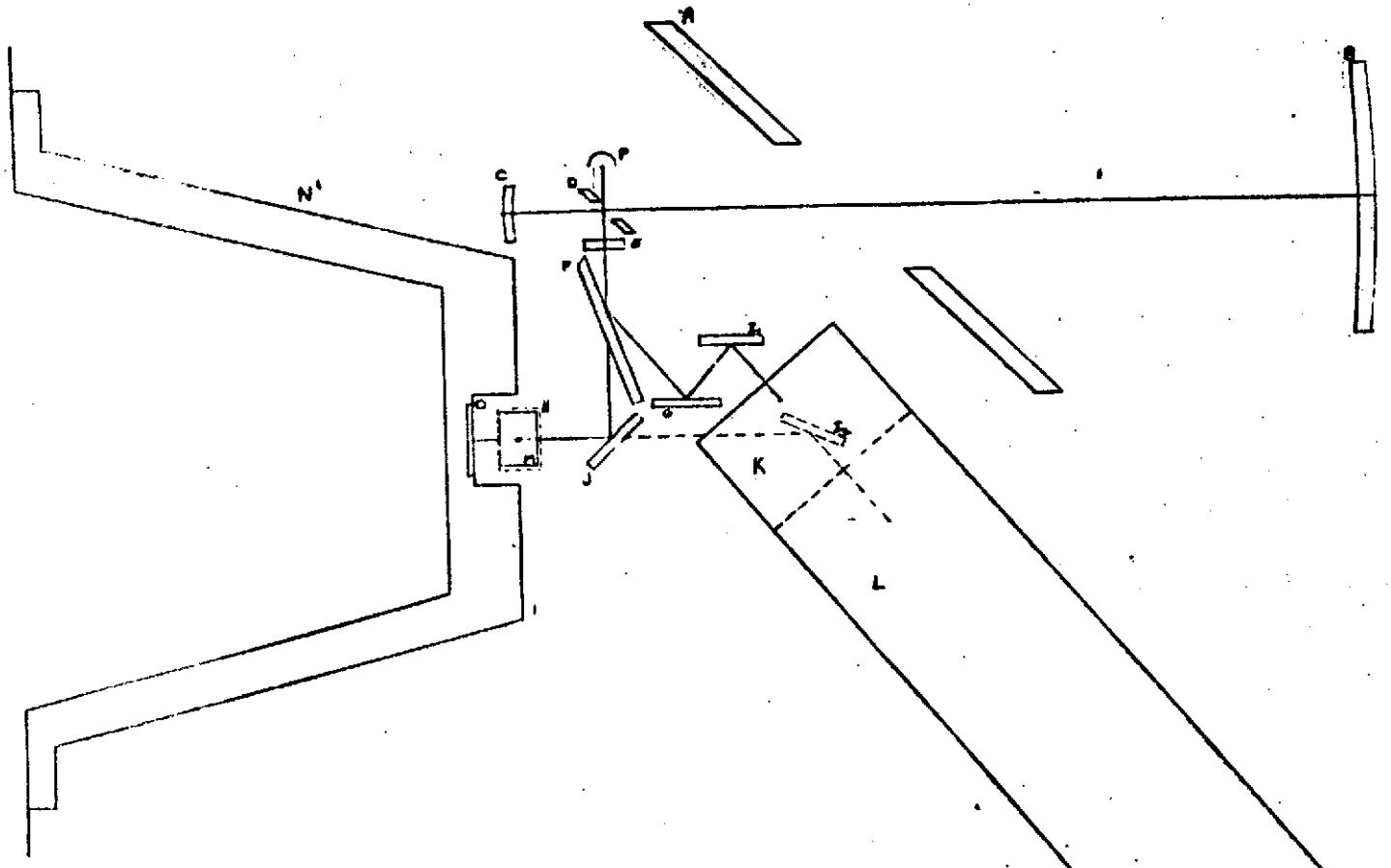

FIGURE 2.

TABLE II

A	POINTING MIRROR	3 3/4 oz	107 g
B	PRIMARY MIRROR	1 oz	28 g
C	SECONDARY MIRROR	1/4 oz	7 g
D	FOCAL PLANE FOLDING MIRROR	1/4 oz	7 g
E	RETARDATION PLATE	1/4 oz	7 g
F	BREWSTER ANGLE BEAMSPLITTER	2 oz	57 g
G	TRANSMITTER SCANNING MIRROR	1 1/2 oz	43 g
H	HOLOGRAPHIC BEAM FOCUSSER	1/2 oz	14 g
I_1, I_2	STATIONARY FOLDING MIRRORS	1/4 oz each	14 g
J	RECEIVER SCANNING MIRROR	1 1/2 oz	43 g
K	TRANSMITTING LASER		
L	LO LASER		
M	MIXING BEAMSPLITTER	1/2 oz	14 g
N	RADIATION COOLER	3 lb	1360g
O	DETECTOR ARRAY		
P	DETECTOR FOR FEEDBACK LOOP AND CLOCK		

TABLE III

SURFACE	RADIUS OF CURVATURE (mm)	AXIAL THICKNESS (mm)	INDEX OF REFRACTION	FREE APERTURE (mm)	HOLE DIAMETER (mm)
1	OBJECT	∞	1 (VACUUM)		
2	∞	135.	-1 (POINTING MIRROR)	107. (AXIS)	36.5 (AXIS)
3	-420.	-210.	1 (PRIMARY MIRROR)	76.3	
4	∞	-25.2	1 (FOCAL PLANE MIRROR)	7.7 (AXIS)	3.8 (AXIS)
5	30.48	25.2	-1 (SECONDARY MIRROR)	13.3	
6	IMAGE				

CONIC CONSTANTS

SURFACE 3 -.82

SURFACE 6 -.45

TABLE IV

COMPONENT (SEE FIG. 1)	MODE	OPTICAL EFFICIENCY
A	REFL	.782 (.992 reflective, .79 geometric)
D	REFL	.743 (.992 reflective, .75 geometric)
B, C, G, I_1, J	REFL	.992
E	TRANS	.960
F	REFL	.779
F	TRANS	.990
M	TRANS	.990

SCAN MECHANISM

The solid angle to be scanned is roughly a square of 5°x5°. Because of limitations in the telescope optics (a maximum field angle of 1°) the square will be divided into five strips, 1°x5° each, to be scanned consecutively.

A high-speed linear scan has to be generated before the telescope (magnification $m \tilde{=} 10$); thus an oscillating mirror would have to have an excursion of $\frac{1° \times 10}{2} = 5°$ peak-to-peak to generate the fast scan. The transverse component of the scan is provided by a slow motion of the pointing mirror.

The requirements on the fast scanner led to the selection of a matched pair of high-speed torsional tuning forks: a mirror carried on each fork is used in transmission and reception, respectively. The two forks are exactly matched in frequency: one fork is free-running at its normal frequency; the second fork is electronically slaved to the first one. Amplitudes of oscillation are similarly matched by the comparison of velocity sensing signals and the use of error feedback. Finally, by means of an electrically adjustable phase-shifting network, the phase difference between the oscillating mirrors can be accurately adjusted during the detection and tracking modes: this capability is required to compensate for the finite round-trip delay of the laser pulse.

THEORY OF THE SCAN

Let the mirror oscillating frequency be f, and $\omega=2\pi f$;

A, the amplitude of oscillation,

ϕ, the phase difference.

The mirror angles are:

$\theta_1 = A \sin \omega t$ (transmit)

$\theta_2 = A \sin (\omega t-\phi)$ (receive)

The mirror scanning speed $\dot{\theta}$ is:

$|\dot{\theta}_1| = |\dot{\theta}_2| = \omega A$

The magnification of the optics is M, and the directions of the transmitted and received beams θ_T and θ_R are given by:

$$\theta_T = \frac{2}{M} A \sin \omega t$$

$$\theta_R = \frac{2}{M} [A \sin (\omega t-\phi)]$$

For a given transmitted pulse, the constraint is

$$\theta_T = \theta_R ,$$

but these angles have to be generated at different times, separated by $\Delta t = \frac{2R}{c}$, where R is the range to target,

c is the velocity of light.

This constraint can be expressed by the equation

$$\theta_T(t)=\frac{2}{M}A\sin\omega t=\theta_R(t+\frac{2R}{c})=\frac{2}{M}A\sin[\omega(t+\frac{2R}{c})-\phi]$$

or $$A\sin\omega t=A\sin[\omega(t+\frac{2R}{c})-\phi]$$

The constraint is satisfied if:

$$\phi(R) = \frac{2R\omega}{c} \text{ modulo } 2\pi$$

Once a target has been detected and is being range-tracked, the phase ϕ can be tracked to maintain the reflected light spot centered on a particular detector of the receiving array. In such a tracking implementation the quantity $\phi(R)$ is varied linearly with R, with discontinuities of 2π.

Prior to detection however, the range uncertainty corresponds to a spread in the value of ϕ ;

$$\phi(R_o \pm \Delta R) = \phi(R_o) \pm \Delta\phi;$$

$$\Delta\phi = \frac{2R\omega}{c} \text{ modulo } 2\pi$$

For a range uncertainty ΔR=15 nautical miles (at R_o=300 nautical miles), and f=600 Herz, the above expression yields $\Delta\phi \cong .7$ radian.

For the magnification M=10,

and for A=2.5° (mechanical the receiving angles are spread over the interval:

$$\theta_2 \pm \Delta\theta_2 = A\sin(\omega t - \phi_o \pm .7 \text{ radian})$$

The largest spread in values of the receiving scan mirror angle θ_2, obtained by maximizing $\Delta\theta_2$, is:

$$\Delta\theta_2 = \frac{A}{2}\left|\sin(\omega t - \phi_o + .7 \text{ rad}) - \sin(\omega t - \phi_o - .7 \text{ rad})\right|$$

$$= \frac{A}{2}[2\cos(\omega t - \phi_o)\sin .7 \text{ rad}]$$

$$(\Delta\theta_2)_{max} = A\sin(.7\text{rad}) = 2.5°\sin .7\text{rad}$$

$$= 1.75° \text{ mechanical.}$$

To assure reception, a multiplicity of detectors is used, aligned in the direction of the fast scan, and subtending an angle

of $2(\Delta\theta_2)_{max}$ at the receiving scan mirror. The distance D between the second scan mirror and the detector array is 1.5" in the optical design layout. Thus, for a fast scan frequency of 600 Herz, the length of the detector array is $2(\Delta\theta_2)_{max} \times D = 2.3$ millimeters. Such an array can be realized by 6-7 elements of a diameter of 200 μm each, spaced by 200 μm.

There is a possible trade-off between the scanning speed $\dot{\theta}$ and the number of detectors in the array.

DOCKING

THE PROBLEM

When a space tug has detected a satellite and performed a preliminary approach and positioning maneuver prior to docking, there remains the problem of accurate alignment of the two spacecraft. An optical docking sensor and technique are described below, which permit tug control for accurate alignment and finalapproach.

DESCRIPTION

Figure 3 shows a side view of the satellite, as well as a view of the tug. The axis of the tug intersects the mating face of the satellite at a point distant by r from the satellite axis. This distance r will be referred to as the radial misalignment. The axes of the two spacecraft are, in general, not coplanar.

The required maneuvering consists of three phases which may be accomplished simultaneously and/or sequentially:

a. The reduction to an acceptable value of the radial misalignment r.

b. The reduction to an acceptable value of the angle θ between the axes of the two spacecraft.

c. The reduction to zero of the distance R between the mating faces.

The sensor comprises:

1. An optical transmitter/receiver (not illustrated) located on the tug, which projects a light beam in front of the tug. By means of a scanning mechanism, the light beam is allowed to describe a cone, centered about the tug axis, and having a semi-cone angle β. The transmitter and scanner can be same as are used for satellite detection. The receiver, in this case, has a fixed orientation, a wide aperture and uses direct detection by a diode operating at ambient temperature.
2. A special circular target, shown in Figure 4, centered on the mating face of the satellite. the target consists of two concentric sections: the main section is an annulus A, whose reflectivity depends only on the distance r from the center of the target, being a maximum for small values of r, and a minimum for larger values. Specifically, the reflectivity $\eta(r)$ can be written:

$$\eta(r) = ke^{-ar}$$

This can be achieved by a series of narrow concentric annular zones, alternately of very high and very low reflectivity; the ratio of the widths of two adjacent zones is appropriately tapered as a function of r. The maximum width of a zone is such that it constitutes a small fraction of the diameter of the light spot on the target.

The second section, B, is a small circular area whose surface has a backscattering pattern of low amplitude; this pattern, which is a function of the angle of incidence only, is sharply peaked about normal incidence. Such a surface is being experimentally investigated.

If, as a result of a conical scan of semi-cone angle β, the light beam paints a circle of radius r' on section A of the target ($r \neq o$, $\theta = o$), the reflected power will fluctuate between a maximum and a minimum value, corresponding to distances from the center of the target $r-r'$ and $r+r'$, respectively. The ratio of the maximum and minimum reflected powers will be:

$$\frac{ke^{-a(r-r')}}{ke^{-a(r+r')}} = e^{2ar'},$$

a quantity independent of the radial misalignment r, but dependent on the radius r' of the painted circle.

RANGE SENSING

The range, or distance between the sensor and the target, can now be sensed by adjusting the scan angle β so that the ratio of maximum and minimum reflected powers equals a known value A,

$$A = e^{2ar_o},$$

i.e., so that the radius of the painted circle equals r_o.

From the geometry, the range R is given by

$$R = \frac{r_o}{\beta(\text{radians})}$$

In general, the figure painted or the target will be an ellipse of small eccentricity (for an angular misalignment $\theta = 15°$, the ratio of the semi-minor and semi-major axes a and b equals $\cos 15° = 0.966$) so that the value of range obtained from the above measurement will be in error by a few percent. The accuracy of the measurement improves, however, as

1. the angular misalignment θ decreases, which decreases the eccentricity of the ellipse; and

2. as the range R decreases, since the required cone angle β will be larger, while the noise or uncertainty in β remains a constant.

SENSING OF RADIAL MISALIGNMENT

The direction and sense of the radial misalignment are derived from a knowledge of the scan coordinates ϕ_{max} or ϕ_{min} (the scan spin angles at the moments of maximum or minimum reflected power). See Figure 5.

The required correction is a rotation of the tug about the axis $\bar{\rho}$, in a right-hand screw convention.

In general, a sequence of such corrections will cause the center of the painted ellipse to approach the center of the target not in a straight line, but in a very slightly curved line, as shown in Figure 5b.

The magnitude of the required correction is not known. But, as the radial misalignment r is reduced to a small value, the sensor illuminates increasing portions of the central circular area of the target face, section B. The low reflectivity of section B causes increasingly long dips to appear at the output of the light detector, signalling the approaching end of the radial correction phase. That phase is ended when the entire conical scan falls into section B.

SENSING OF ANGULAR MISALIGNMENT

Here again, in each scan period, there will be a point of maximum and a point of minimum backscattered light power, as illustrated in Figure 6a. For a given angular misalignment θ, the ratio of maximum to minimum sensor outputs will be larger at smaller ranges, which is desirable. As the value of θ decreases, the fluctuations in sensor output decrease and finally remain at a uniform level (Figure 6b).

The required correction is known in direction and sense, as was the case for the correction of radial misalignment: it is a rotation of the tug about an axis $\bar{\psi}$ in the plane of the target. In addition, the magnitude of the required rotation can be approximately calculated from the known backscattering pattern of the surface of section B.

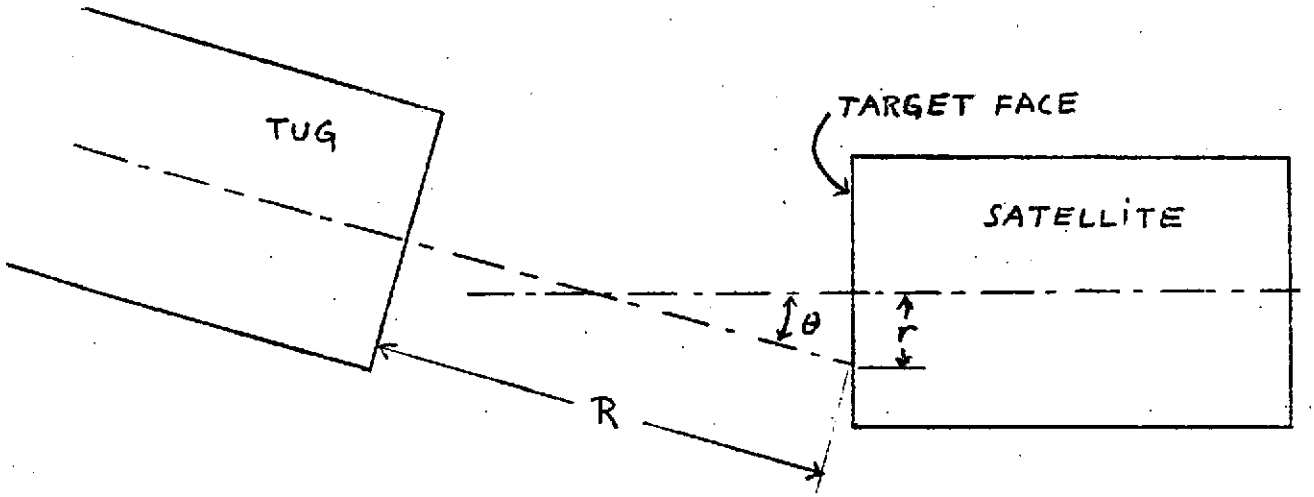

r : radial misalignment
θ : angular misalignment
R : range

Fig. 3 TUG & SATELLITE, SIDE VIEW.

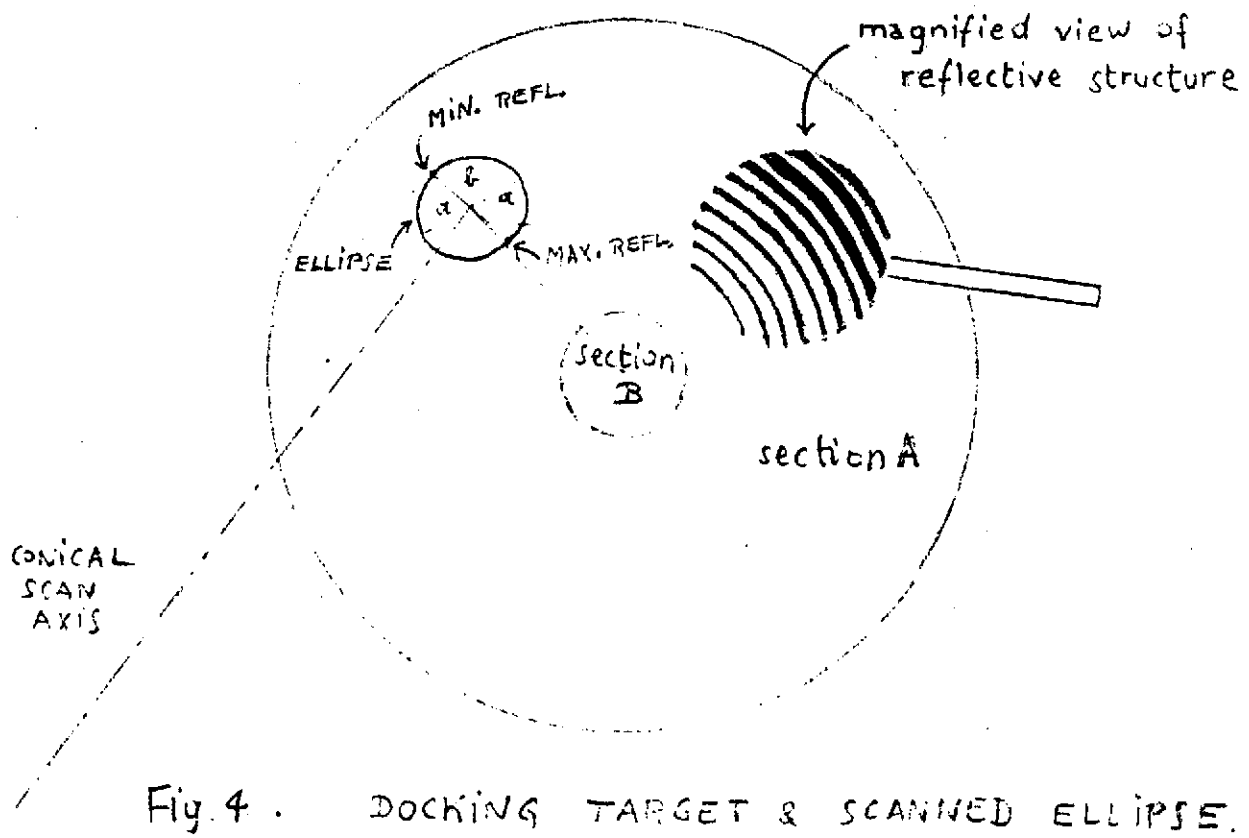

Fig. 4. DOCKING TARGET & SCANNED ELLIPSE.

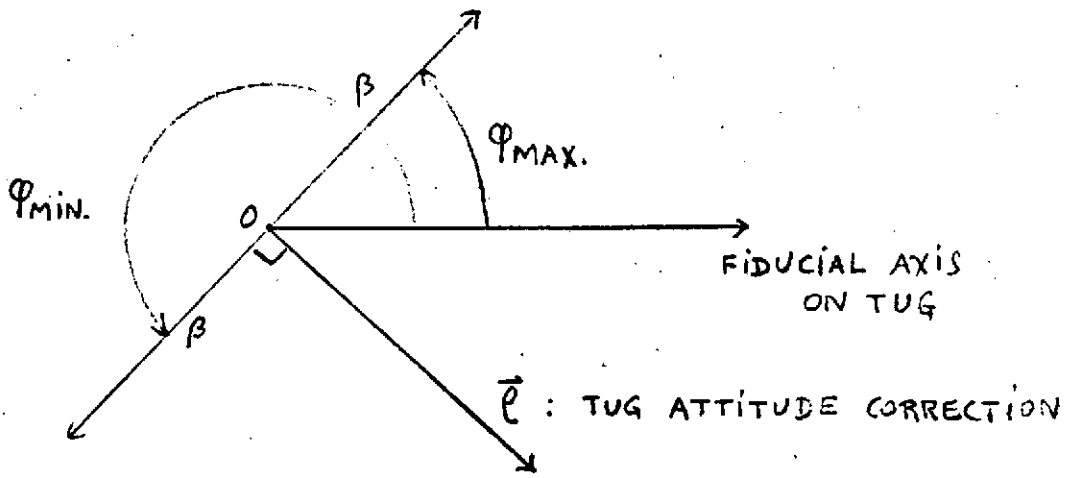

SCAN AXIS : O, into plane of paper
SCAN COORDINATES : β, semi-cone angle
φ, spin angle

Fig. 5a CORRECTION OF RADIAL MISALIGNMENT.

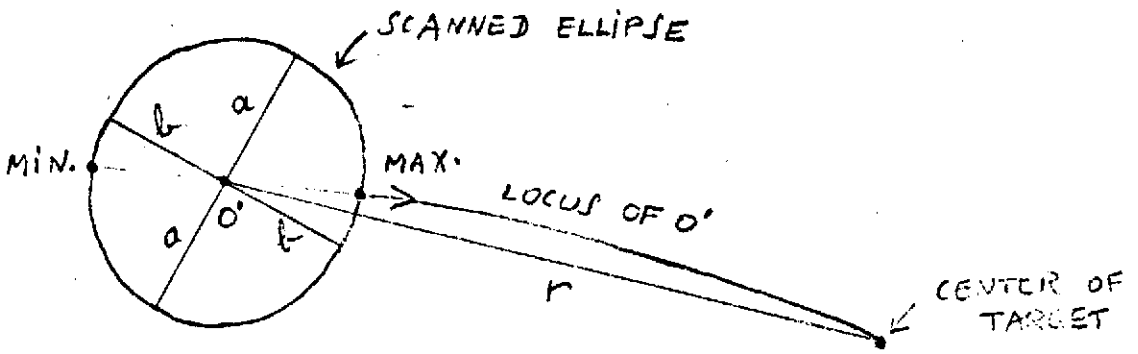

Fig. 5b MOTION OF SCANNED ELLIPSE DURING CORRECTION OF RADIAL MISALIGNMENT.

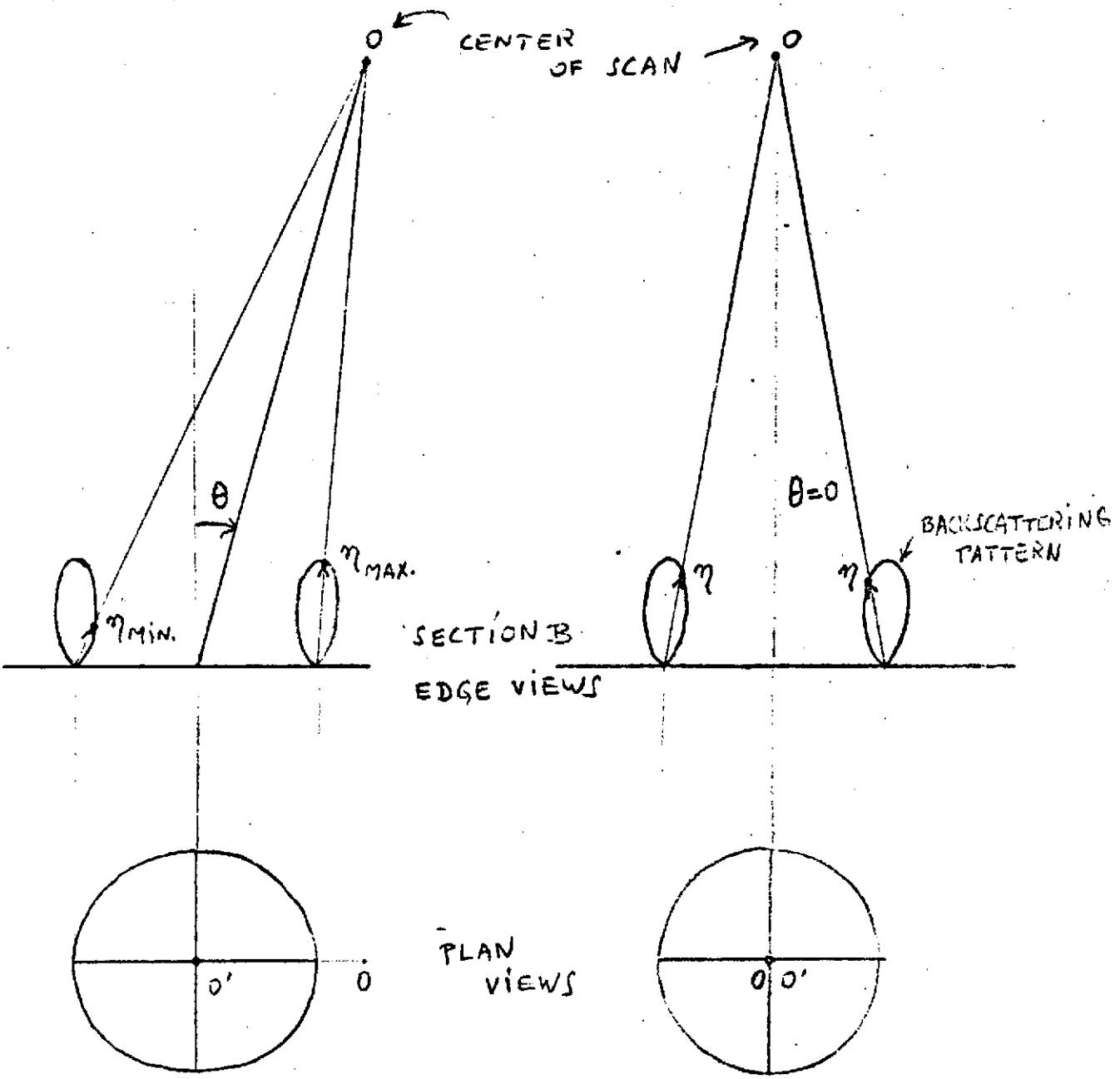

Fig. 6a

Fig. 6b

POWER BACKSCATTERED FROM SECTION B, AT TWO OPPOSITE POINTS OF SCAN.

$\theta \neq 0$: POWER FLUCTUATES

$\theta = 0$; POWER = CONSTANT.

SEQUENCING OF CORRECTIONS

As the alignment proceeds the three sensing modes and the subsequent corrections can be sequenced: initially the sensing of R and r, and finally the sensing of R and θ. This latter sequence is obtained by deliberate offsets of the scan axis to alternate between conical scans in sections A and B.